# Methane Partitioning and Transport in Hydrated Carbon Nanotubes

**Amrit Kalra,[†,‡,§] Gerhard Hummer,[*,‡] and Shekhar Garde[*,†]**

*The Howard P. Isermann Department of Chemical and Biological Engineering, Rensselaer Polytechnic Institute, 110 Eighth Street, Troy, New York 12180, and Laboratory of Chemical Physics, Building 5, National Institute of Diabetes and Digestive and Kidney Diseases, National Institutes of Health, Bethesda, Maryland 20892*

*Received: June 26, 2003; In Final Form: October 17, 2003*

The well defined shape and size of carbon nanotubes (CNTs) makes them attractive candidates for theoretical and experimental studies of various nanoscopic phenomena such as protection and confinement of molecular species as well as transport of molecules through their interior pores. Here we investigate solute partitioning and transport using molecular dynamics simulations of CNTs in mixtures of hydrophobic solutes and water. The hydrophobic pores of CNTs provide a favorable environment for partitioning of hydrophobic solutes. We find that the transfer of a methane molecule from aqueous solution into the CNT interior is favored by about 16 kJ/mol of free energy. In 50 molecular dynamics simulations, we observe that methane molecules replace water molecules initially inside the nanotubes, and completely fill their interior channels over a nanosecond time scale. Once filled with methane molecules, the nanotubes are able to transport methane from one end to the other through successive methane uptake and release events at the tube ends. We estimate a net rate of transport of about 11 methane molecules per nanotube and nanosecond for a 1 mol/L methane concentration gradient. This concentration-corrected rate of methane transport even exceeds that of water through nanotubes (∼1 per nanosecond at a 1 mol/L osmotic gradient). These results have implications for the design of molecule-selective CNT devices that may act through mechanisms similar to those of biological transmembrane channels.

## I. Introduction

Carbon nanotubes[1] or nanopores made of other materials constitute ideal model systems to study the unique properties of fluids in confined systems,[2−7] such as wetting, selective partitioning, and transport of solution species in a quasi one-dimensional geometry.[3,8−10] Following a theoretical prediction of nanotube filling with small molecules,[11] several experimental studies have investigated nanocapillarity-induced filling processes. In particular, wetting of the exterior and interior of nanotubes by low-surface-tension liquids[12] and nanotube filling by metal[13−15] and nonmetal[16] atoms has been studied. Recently, filling of nanotubes by potassium-iodide nanocrystallites was observed experimentally[17] and in simulations.[18] Gas adsorption on the outer surfaces of capped nanotube bundles[19] and into open as well as capped single-walled nanotubes[20] has been studied experimentally. Novel applications of nanotubes in detection of surrounding liquid motion[21,22] and laser-driven atomic transport[23] have also been explored.

Structural and hydrogen bonding properties of water in nanotubes have been investigated by molecular dynamics (MD) simulations.[5,6] Other MD simulation studies suggest the formation of methane nanohydrates[24] and of new ice phases[25] in nanoscopically confined spaces. Recent MD simulations also showed the filling of an open-ended nanotube by water and subsequent transport of water through the nanotube.[3] Weakening of the attractive nanotube-water interactions resulted in sharp two-state like transitions between water-filled and empty states. In the filled state, a hydrogen-bonded water wire was found to span the interior of the nanotube. Water was indeed observed experimentally inside narrow single-wall open CNTs[26] and large multiwall capped CNTs.[27,28]

The MD simulations of water filling under equilibrium conditions[3,8] suggest exciting possibilities for the use of nanotubes in selective partitioning of solutes from mixtures or solutions. For example, unfavorable free energies of solvation of hydrophobic solutes in bulk water phase should provide a strong thermodynamic driving force for their partitioning into the nanotube interior. Here we report MD simulations of short open-ended carbon nanotubes in aqueous solutions of hydrophobic solutes. We study thermodynamic, structural, and kinetic aspects of the hydrophobically driven filling of carbon nanotubes with methane molecules through fifty independent MD simulations. Once filled with methane, we observe a dynamic exchange of interior methane molecules with those on the outside. Concerted events of this kind lead to a selective transport of methane molecules through the nanotube. A kinetic analysis of such transport events is presented.

The paper is organized as follows. The simulation setup and computational details are described in section II. In section III, we present structural and thermodynamic aspects of methane partitioning into the nanotube, followed by an analysis of the transport of methane through the nanotube. Conclusions are drawn in section IV.

## II. Methods and Simulation Details

**Simulation Setup.** In the fifty separate MD simulations performed here, each setup includes three components: an open-

* Corresponding authors. E-mail: gardes@rpi.edu (http:// www.rpi.edu/∼gardes), hummer@helix.nih.gov

† Rensselaer Polytechnic Institute.

‡ National Institutes of Health.

§ Present address: Department of Chemical Engineering, Massachusetts Institute of Technology, 77 Massachusetts Avenue, Cambridge, MA 02139.

10.1021/jp035828x CCC: $27.50 
Published on Web 12/17/2003

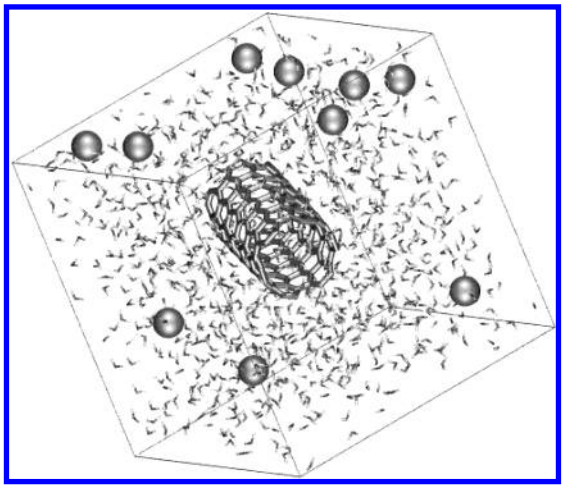

**Figure 1.** Snapshot of the simulation system at the start of an MD run (image created using Visual Molecular Dynamics package).[53] Ten methane molecules (spheres) are placed at least 12 Å away from any atom of the carbon nanotube. Water molecules are shown in a wireframe representation.

**TABLE 1: Partial Charges and Atom−Atom Lennard-Jones Interaction Parameters ($\epsilon$ and $\sigma$)**

| atom | $q$/e | $\epsilon$, kJ/mol | $\sigma$, Å |
|---|---|---|---|
| C (nanotube) | 0.00 | 0.36 | 3.40 |
| $CH_4$ (methane) | 0.00 | 1.23 | 3.73 |
| O (TIP3P $H_2O$) | −0.834 | 0.64 | 3.15 |
| H (TIP3P $H_2O$) | 0.417 | 0.00 | 0.00 |

ended carbon nanotube, solvent water, and methane solutes. We used a (6,6) armchair-type carbon nanotube (see Figure 1) that comprises 144 $sp^2$ carbon atoms,[29] similar to the one studied in ref 3. The length and diameter of the tube (center-to-center distance between relevant carbon atoms) are 13.4 and 8.1 Å, respectively. Methane molecules are represented as spherically symmetric united-atom Lennard-Jones solutes.[30] The TIP3P model[31] is used for water with Lorentz−Berthelot mixing rules for Lennard-Jones interactions. Table 1 lists the Lennard-Jones parameters and partial charges for molecules used in this study.

Our goal was to study partitioning of methane molecules into CNTs, and transport of methane through CNTs. To achieve this, we generated 50 initial configurations in which one CNT and ten methane molecules were placed randomly into a preequilibrated box of water. Water molecules that overlap with the CNT or with methane molecules were removed. A few additional water molecules were removed randomly such that each starting configuration contained a total of 1024 water molecules. To study the hydrophobically driven filling of CNTs, methane molecules in the initial configurations were placed at least 12 Å away from any CNT atom. Fifty independent MD runs were started from these initial configurations. A snapshot of a typical initial system configuration is shown in Figure 1.

MD simulations were performed using AMBER 6.0[32] at constant temperature and pressure of 300 K and 1 atm, respectively.[33] Periodic boundary conditions were applied with particle-mesh Ewald electrostatics.[34] A time step of 2 fs was used, with water bond lengths constrained by SHAKE.[35] Each of the 50 initial configurations was equilibrated for 100 ps. Simulations were run for at least 2−3 ns following the equilibration, or until the complete filling of the nanotube. Configurations were saved every picosecond for further analysis. Ten of these fifty simulations were run significantly longer (approximately 10 ns each) to study the transport of methane solutes through methane-filled CNTs. The total simulation time in fifty simulations amounts to approximately 220 ns.

**Analysis of Filling of the Nanotube with Methane Molecules.** The filling process was monitored by calculating the number of methane molecules, $n(t)$, that have partitioned into the nanotube as a function of time. In a typical filling process, $n(t)$ goes up from zero at the beginning of the simulation to four or five when the tube is completely filled. There is some ambiguity in defining precisely the boundary between the region "inside" and "outside" of the nanotube. For example, if we identify a coaxial cylindrical volume[36] of radius 2 Å and length $L = 14.6$ Å as being "inside" the tube, then instantaneous back and forth movements of methane molecules located at the boundary lead to rapid fluctuations in $n(t)$ with time. To smooth these fluctuations, a fractional contribution equal to $\exp\{-[(|z| - L/2)/z_0]^2 - (r/r_0)^2\}$ is added to $n(t)$ for methane molecules just outside the cylindrical volume defined by $r < 2$ Å and $|z| < L/2$, where $z_0 = 3.5$ Å, $r_0 = 1.8$ Å. The terms $z$ and $r$ are the axial and radial cylindrical coordinates, respectively, of methane molecules in the reference frame of the nanotube. Here $z = 0$ is at the center of the tube, and $r$ is the distance from the tube axis. The resulting fractional value of $n(t)$ was then changed to the nearest integer number to identify the filling events. Such a procedure reduces the aforementioned ambiguity in assigning the occupancy number.

## III. Results and Discussion

**Filling of the Nanotube with Methane Molecules**. The nanotube is empty at the beginning of each of the fifty simulations. The interior pore of the nanotube is wide enough to hold a single-file arrangement of water or methane molecules. Indeed, the initially empty nanotube gets filled rapidly with water during the equilibration run, as observed in ref 3. The structural, kinetic, and energetic aspects of this water chain have been discussed in detail elsewhere.[3,8,37] As simulations proceed, methane molecules in the aqueous methane−water mixture sample the region near open ends of the nanotube. This results in breaking of the hydrogen-bonded water wire and subsequent partitioning of the first methane molecule into the nanotube, driven by a large thermodynamic driving force, as shown below. As time progresses, the remaining water molecules in the nanotube are pushed out by newly entering methane molecules, resulting in a nanotube that is completely filled by methane.

Figure 2 shows a typical sequence of events leading to the filling of a nanotube with four methane molecules as monitored by $n(t)$. In that run, the first methane molecule enters the nanotube after about 700 ps, and filling is completed on a nanosecond time scale. In general, the time required for methane to partition into the nanotube can be divided roughly into two parts. First, methane molecules diffuse near the nanotube ends, requiring an average time $\tau_d$; second, a vicinal methane molecule enters the nanotube after an average time $\tau_{entry}$. The former time will depend on the concentration and diffusion coefficient of methane (as estimated below). The latter time will depend on the structural details of the hydration of nanotube ends which could, in principle, present a barrier for entry of vicinal methane into the tube. Mean first passage times for diffusion into the vicinal region and for entry into the tube were estimated from the trajectories of fifty independent MD simulations. We defined hemispherical regions of radius $R^* = 6$ Å from the nanotube ends as the vicinal region. As stated earlier, methane molecules were placed at least 12 Å away from any of the nanotube atoms in the starting configuration. Therefore, the value $\tau_d$ for the first methane to sample the vicinal region (~450 ps) is somewhat higher than the average diffusion times for subsequent methane

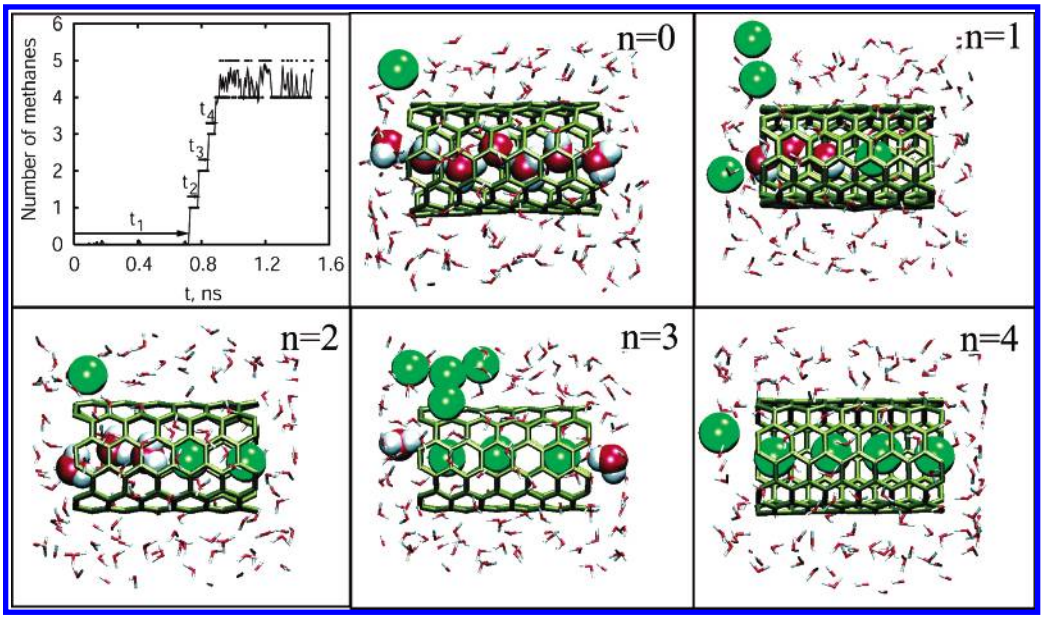


**Figure 2.** Time-dependent filling of the nanotube, quantified by the number $n(t)$ of methane molecules in the tube (top left panel). Both fractional (line) and nearest integer values of $n(t)$ (dots) are shown. The other five panels illustrate the sequential filling of methane molecules into the nanotube, where $n$ is the number of methane molecules inside the tube. Only the region near the nanotube is shown for clarity. Methane molecules are shown as spheres, and water molecules are drawn in a space-filled representation (inside the tube) and wireframe representation (outside the tube). The water molecules inside the tube are eventually exchanged with four methane molecules.

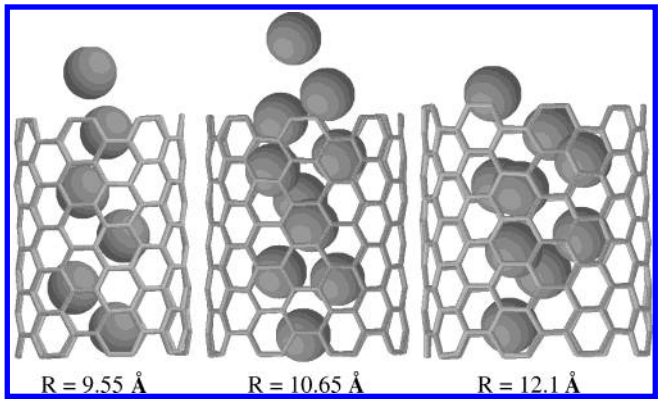


**Figure 3.** Snapshots of methane-filled nanotubes obtained from MD simulation trajectories. Larger nanotubes of diameters 9.55, 10.65, and 12.1 Å fill up with methane molecules, similar to the smaller nanotube (diameter 8.1 Å) used in the present study.

molecules, which are between 100 and 200 ps. These values are in good agreement with the mean time estimated from the diffusion-controlled rate coefficient,[38] $\tau_d \approx (4\pi D_{Me} R^* \rho_{Me})^{-1} \approx$ 100 ps, for a methane density of $\rho_{Me} = 0.3$ nm$^{-3}$ and a methane diffusion coefficient of $D_{Me} = 4.7 \times 10^{-5}$ cm$^2$ s$^{-1}$ in TIP3P water.[39] From the vicinal region, entry of methane molecules into the nanotube occurs rapidly, with $\tau_{entry}$ being approximately 10 ps.

We performed additional simulations to probe the effects of nanotube pore size and nanotube−water attractive interactions on the methane partitioning process. We find that methane also partitions into nanotubes with wider pores, as shown in Figure 3. However, in these wider tubes, methane molecules do not form the single-file arrangement observed in the (6,6) tube. Methane filling also occurs if the nanotube−water attractive interactions are reduced to a level in which the (6,6) tube in pure water fluctuates between water-filled and empty states.[3] An analysis of the limited kinetics data for nanotubes with reduced carbon−water attractions suggests that filling even accelerates, as one would expect if the displacement of water from the tube interior is a rate-determining factor.

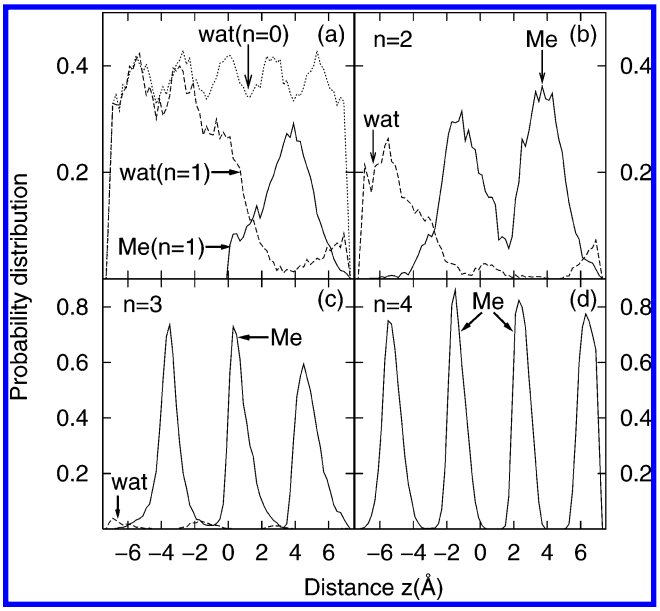


**Figure 4.** Axial densities of water (dashed lines) and methane molecules (solid lines) in the nanotube. Results for $n = 1$, 2, 3, and 4 methane molecules inside the tube are shown in panels (a), (b), (c), and (d), respectively. Panel (a) also shows the water density profile for a water-filled tube ($n = 0$).

**Structural Features of the Filling Process.** We also monitored the process of nanotube filling structurally. Figure 4 shows axial density distribution functions of methane and water molecules inside the nanotube for different filling states, normalized by the number of molecules inside the tube. To preserve the inherent symmetry about $z = 0$ in this system, the direction of the positive $z$ axis for a given configuration is determined by the center of mass of methane molecules in the nanotube.

At the beginning of MD simulations, methane molecules are away from nanotube atoms and the tube gets rapidly filled with 5−6 water molecules that form a single-file hydrogen-bonded wire spanning the length of the nanotube. The preferred locations

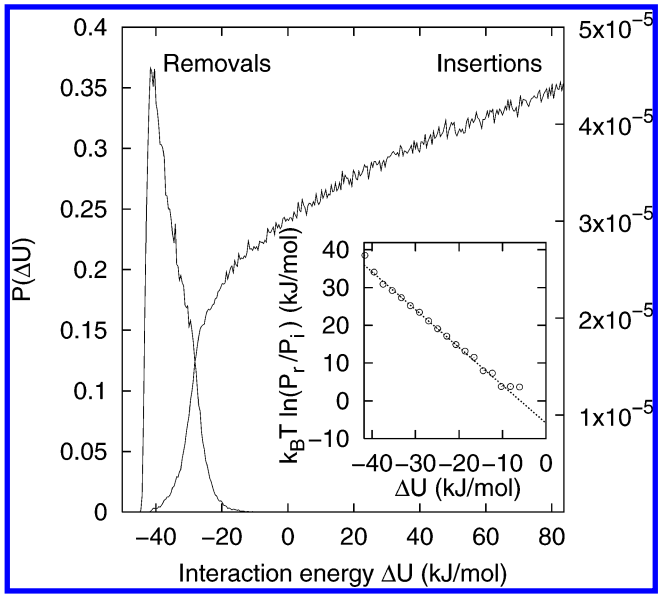


**Figure 5.** Probability distributions for energies of insertion/removal of a methane molecule into/from the nanotube. The probability scales for removals and insertions are on the left and right, respectively. The symbols in the inset show $k_BT \ln[P_r(\Delta U)/P_i(\Delta U)]$ versus $\Delta U$ with a linear fit of slope $-1$ (dotted line).

of these water molecules inside the nanotube appear as peaks in Figure 4a that are separated by 2.8 Å. The peaks are broad and overlap, indicating significant positional fluctuations of the water wire as a whole.[40] The first methane molecule that enters the nanotube prefers locations near the end of the nanotube, as seen in the peak in methane density at $z \approx 4$ Å in Figure 4a. The remaining tube is filled with three water molecules on average. Entry of the second methane reduces the number of water molecules in the nanotube to approximately one (Figure 4b). Subsequent transitions to states $n = 3$ and 4 (panels c and d of Figure 4) push the remaining water molecule out of the nanotube. In tubes completely filled with methane, the positions of methane molecules are more sharply defined than those of water molecules in the hydrogen bonded wire. Trapping of water molecules between two methane molecules is rare, as shown by small water density peaks flanked by methane density peaks in panels b and c of Figure 4.

**Thermodynamics of Methane Partitioning.** The spontaneous partitioning of methane molecules into the carbon nanotube described above is driven by a favorable free energy. We calculated the excess chemical potential of a methane molecule inside a filled nanotube by Bennett's method of overlapping energy distributions.[3,41] Trial insertions and removals of methane molecules were performed after the nanotube was completely filled with four methane molecules. A total of approximately 22 ns of simulation data on filled nanotubes were used for these calculations.

Figure 5 shows probability distributions of methane insertion and removal energies, $P_i(\Delta U)$ and $P_r(\Delta U)$, with removals and insertions restricted to a coaxial cylindrical volume of radius 2 Å and length 14.6 Å. Because the tube is predominantly filled with methane molecules, successful insertions can be made rarely. However, for successful insertions, energies as low as $-40$ kJ/mol are observed. The observed removal energies of methane molecules are always negative, typically below $-20$ kJ/mol. The logarithm of the ratio of probabilities, $k_BT \ln[P_r(\Delta U)/P_i(\Delta U)]$, shown in the inset of Figure 5, varies linearly with $\Delta U$ with a slope of $-1$, indicating thermal equilibrium.[41] $k_B$ is Boltzmann's constant, and $T$ is the absolute temperature. The intercept of $-5.9$ kJ/mol is equal to the excess chemical potential of a methane molecule inside the nanotube. Previous simulation studies provide a value of approximately 10.5 kJ/mol for the excess chemical potential of united atom methane in bulk water.[42,43] Partitioning of a single methane molecule from bulk water phase into the nanotube is therefore favored by about 16.4 kJ/mol (more than 6 $k_BT$ at room temperature). These calculations highlight a significant thermodynamic driving force for hydrophobic solute partitioning from water into an open-ended carbon nanotube. We note, however, that a sufficiently high concentration of methane in the solution is required for methane to compete with water for complete filling of the nanotube. We estimate that concentration roughly from $\rho_w \exp[-(\Delta\mu_w^{ex} - \Delta\mu_{Me}^{ex})/k_BT] \approx 0.3$ mol/L, where $\rho_w \approx 55$ mol/L is the concentration of bulk water, $\Delta\mu_{Me}^{ex} \approx -16.4$ kJ/mol is the difference in excess chemical potentials between the nanotube and bulk water, and $\Delta\mu_w^{ex} \approx -3.43$ kJ/mol is the corresponding value for water.[3] Under a 1-bar methane atmosphere, the methane concentration in water is far lower, approximately equal to $10^{-3}$ mol/L, reflecting the low solubility of methane in water. In light of the above discussion, the probability of observing states with $n = 0$, 1, 2, 3, or 4 methane molecules will depend on the outside methane concentration. At low methane concentrations, the nanotube may only be partially filled on average.

**Methane Transport Through the Nanotube.** Once the nanotube is filled, the probability of methane molecules to be replaced by water molecules is vanishingly small due to a significant thermodynamic bias for methane partitioning. Indeed, the number of methane molecules rarely drops from $n(t) = 4$ to 3 in the simulations. However, exchanges between methane molecules inside and outside the nanotube occur frequently. In a typical exchange event, a methane molecule from outside enters the nanotube from one end and simultaneously pushes out another methane molecule at the other end of the tube as seen before for water.[3,40] Several such exchanges are observed in the simulations of methane-filled nanotubes. As a result, transport of a methane molecule along the length of the nanotube via a concerted sequence of such events is possible. Over a simulation time of roughly 100 ns, about 66 translocation events are observed in which a methane molecule entering from one end of the nanotube exits at the other end. Importantly, the transport is selective because once the initial water molecules are replaced by four methane molecules, water molecules do not re-enter the tube in significant numbers. Clearly, selectivity for methane transport through the nanotube is a result of the high thermodynamic bias for partitioning of methane molecules into the tube relative to that of water. This underlying principle of selective partitioning leading to selective transport is also likely relevant for biomolecular channels that are designed to transport low-concentration solutes across physical barriers, such as membranes. For example, a glycerol channel[44] has distinct glycerol binding sites to help partition glycerol molecules into the pore as a prerequisite for efficient transport of this low-concentration species. In contrast, a water transport channel is hydrophobic,[45,46] trading off a lower affinity for its high-concentration substrate with high water mobility along the channel.[3,40,47]

We further analyze the kinetics of methane translocation. Figure 6 shows the distribution of methane translocation times measured in simulations of methane-filled nanotubes. The average time for translocation estimated from this distribution is approximately 1.3 ns. That is, on average, it takes approximately 1.3 ns for a translocating methane molecule entering

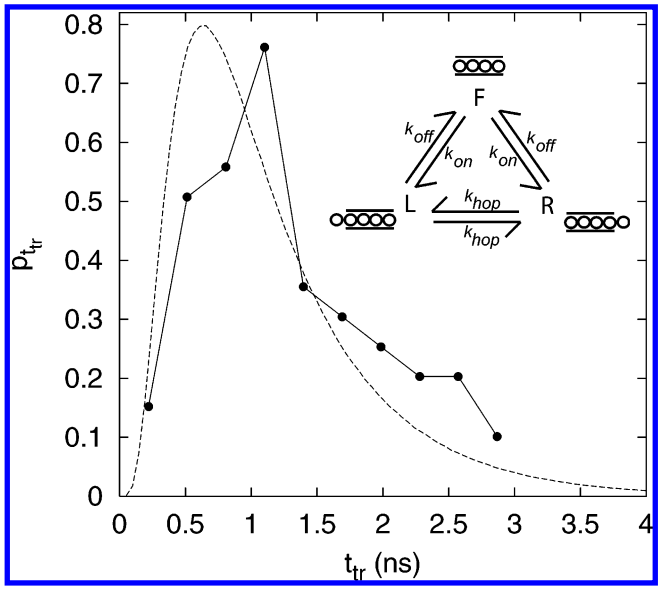


**Figure 6.** Probability distributions for the time required for methane molecules to traverse the length of the tube. Solid and dashed lines represent data from MD and stochastic simulations, respectively. The inset shows the kinetic scheme used for the stochastic simulation. States F, L, and R are represented by a nanotube (two parallel horizontal lines) with four or five methane molecules (open circles) at different positions. $k_{on}$, $k_{off}$, and $k_{hop}$ are the rate coefficients for association, dissociation, and hopping, respectively.

at one end of the tube to exit at the other end. The probability distribution of translocation times can also be estimated using the simple kinetic scheme shown in the inset of Figure 6. As described above, the transport of methane molecules occurs in steps that include (i) the association of an outside methane to a nanotube end, (ii) hopping of the resulting chain of methane molecules along the tube axis which pushes out a methane at the other end, and (iii) dissociation of the methane pushed out. Therefore, our kinetic scheme includes three states that are important for transport: state F characterizes a nanotube filled with four methane molecules without the fifth methane in the vicinity; state L a four-methane-filled nanotube with the fifth methane associated at the left end; and state R a four-methane-filled nanotube with a fifth methane at the right end. States L and R form from state F by association of a methane molecule to the respective end, or by a hopping event from each other. The states are linked by rate coefficients, $k_{on}$, $k_{off}$, and $k_{hop}$ as shown in the kinetic scheme. Of these, the rate coefficient $k_{on}$ is dominated by the diffusion of methane molecules from bulk to the vicinal region and therefore will depend on the bulk methane concentration. For the concentration used here, we measure that rate to be ~1/(100 ps). Once a methane is present at one end of the nanotube, it can either hop inside the tube or dissociate, going back to the bulk solution. We find that the average times for both hopping into or dissociation from the tube are approximately 10 ps, resulting in both $k_{hop}$ and $k_{off}$ to be ~1/(10 ps). Thus, for these values of rate coefficients, it is clear that the availability of methane at the nanotube end by diffusion from bulk to the vicinal region is the slowest step. Once a methane is available, hopping and dissociation occur rapidly.

We performed a stochastic simulation for the kinetic scheme described in the inset of Figure 6 using the estimated values of the rate coefficients. Translocation events can be monitored in this scheme easily. For example, a sequence of concerted F→L→R events can lead to a rightward translocation. The probability distribution for translocation times calculated from the stochastic simulation is in good agreement with that measured in MD simulations, as shown in Figure 6. The stochastic simulation predicts a somewhat shorter average translocation time (~1.15 ns) compared to MD simulations (~1.3 ns). The small discrepancy may reflect in part the limited sampling in the MD simulations. In addition, correlated events are neglected in the stochastic model. In particular, successive methane-release events lead to a buildup of the local concentration of methane molecules, thus biasing the dynamics.

The apparent mobility of methane molecules and the corresponding translocation rate depend on the outside concentration of methane. In case of water transport studied previously,[3,40] the large outside concentration of water leads to an immediate availability of water. As a result, the rate coefficient $k_{on}$ is significantly higher, leading to shorter times for translocation of water (~200 ps) and a higher rate of transport (5−6 water molecules per ns under an osmotic concentration gradient of about 6 M NaCl).[48] To estimate the concentration-dependent rate of methane transport, we modify the model shown in the inset of Figure 6:

$$F_L \underset{k_{off}}{\overset{k\rho_L}{\rightleftharpoons}} L \underset{k_{hop}}{\overset{k_{hop}}{\rightleftharpoons}} R \underset{k\rho_R}{\overset{k_{off}}{\rightleftharpoons}} F_R \qquad (1)$$

with $\rho_L$ and $\rho_R$ being methane concentrations in the large and well-stirred reservoirs $F_L$ and $F_R$ at the left and right of the membrane, respectively. In the steady state, the rate of net methane transport across the membrane is then given by

$$k_{CH_4} = \frac{k(\rho_L - \rho_R)}{2 + k_{off}/k_{hop}} \qquad (2)$$

in units of methane molecules transported per nanotube and unit time. Here, the methane concentrations are $\rho_L = \rho_R \approx 0.3$ mol/L. With an observed rate $k_{on} \approx 1/(100$ ps), we estimate the concentration dependent rate coefficient for methane association to be about $k \approx 33$ (mol/L)$^{-1}$ ns$^{-1}$. With $k_{off} \approx k_{hop} \approx 1/(10$ ps), we thus obtain a rate of about 11 methane molecules transported per nanosecond and nanotube at a methane concentration gradient of 1 mol/L. A quantitative comparison with the gas flux through micrometer-long (10,10) nanotubes under pressure gradient[9] is difficult. First, the actual concentration of methane molecules in aqueous solutions is significantly lower. Second, our simplified treatment for transport through short nanotubes neglects a number of factors, including the formation of gaps in the methane wire,[49,50] the possibility of trapping of water molecules between methane molecules in longer tubes, and the buildup of methane concentration at the membranes. Low solubility is not a problem for other solutes such as methanol for which the behavior of partitioning into the nanotube and transport rates are likely similar to that of methane. Thus, we expect that at sufficient concentrations in solution, a substantial amount of methane or similar hydrophobic molecules may be transported through nanotube membranes, in qualitative agreement with results of Skoulidas et al.[9] Further studies will be required to understand the role of concentration,[48] molecule chemistry, and tube dimensions and chemistry on the ultimate rate of transport.

## IV. Conclusions

Our study shows that small open-ended carbon nanotubes can be used as "molecular straws"[11] to selectively partition hydrophobic molecules into hydrated carbon nanotubes. This partitioning is driven primarily by the free energy of removing hydrophobic solutes from aqueous solution. With methane

molecules fitting neatly inside the (6,6) nanotube, partitioning is driven additionally by favorable van der Waals interactions with the nanotube carbons. Certain quantitative results presented here clearly depend on the details of solute−nanotube and water−nanotube interactions, as discussed in a recent paper.[3] However, the qualitative results on the rapid and favorable filling of a nanotube of suitable geometry from an aqueous solution of gas molecules are general. The results from the present MD simulations suggest an exciting possibility of using nanotubes, in particular nanotube membranes,[47,48,51,52] for selective partitioning of solutes from aqueous solution. The selectivity toward specific molecules may be further enhanced by pore size selection and through nanotube functionalization.

The MD simulations presented here also show that filled nanotubes are able to transport molecules from one end to the other over a nanosecond time scale. Selective partitioning of molecules into a pore leads to their selective transport, as observed here for hydrophobic solutes. This is likely a principle element underlying transport of rare species in molecule selective filters, such as biomolecular channels.[44] With rapidly evolving experimental capabilities for nanotube manipulation, applications of carbon nanotubes in the selective partitioning and transport in nanoscale devices or separation systems should be possible.[51,52]

**Acknowledgment.** S.G. gratefully acknowledges partial financial support of NSF (CAREER award CTS-0134023) and NSF Nanoscale Science and Engineering Center for Directed Assembly of Nanostructures (DMR-0117792). G.H. thanks Prof. J. C. Rasaiah and Dr. A. Berezhkovskii for many stimulating discussions.

## References and Notes

(1) Iijima, S. *Nature* **1991**, *354*, 56.
(2) Gelb, L. D.; Gubbins, K. E.; Radhakrishnan, R.; Sliwinska-Bartkowiak, M. *Rep. Prog. Phys.* **1999**, *62*, 1573.
(3) Hummer, G.; Rasaiah, J. C.; Noworyta, J. P. *Nature* **2001**, *414*, 188.
(4) Beckstein, O.; Sansom, M. S. P. *Proc. Natl. Acad. Sci. U.S.A.* **2003**, *100*, 7063.
(5) Martí, J.; Gordillo, M. C. *Phys. Rev. E* **2001**, *64*, 021504.
(6) Gordillo, M. C.; Martí, J. *Chem. Phys. Lett.* **2000**, *329*, 341.
(7) Maibaum, L.; Chandler, D. *J. Phys. Chem. B* **2003**, *107*, 1189.
(8) Waghe, A.; Rasaiah, J. C.; Hummer, G. *J. Chem. Phys.* **2002**, *117*, 10789.
(9) Skoulidas, A. I.; Ackerman, D. M.; Johnson, J. K.; Sholl, D. S. *Phys. Rev. Lett.* **2002**, *89*, 185901.
(10) Skoulidas, A. I.; Sholl, D. S. *J. Phys. Chem. B* **2002**, *106*, 5058.
(11) Pederson, M. R.; Broughton, J. Q. *Phys. Rev. Lett.* **1992**, *69*, 2689.
(12) Dujardin, E.; Ebbesen, T. W.; Hiura, H.; Tanigaki, K. *Science* **1994**, *265*, 1850.
(13) Ajayan, P. M.; Iijima, S. *Nature* **1993**, *361*, 333.
(14) Ajayan, P. M.; Stephan, O.; Redlich, P.; Colliex, C. *Nature* **1995**, *375*, 564.
(15) Ugarte, D.; Chatelain, A.; de Heer, W. A. *Science* **1996**, *274*, 1897.
(16) Fan, X.; Dickey, E. C.; Eklund, P. C.; Williams, K. A.; Grigorian, L.; Buczko, R.; Pantelides, S. T.; Pennycook, S. J. *Phys. Rev. Lett.* **2000**, *84*, 4621.
(17) Meyer, R. R.; Sloan, J.; Dunin-Borkowski, R. E.; Kirkland, A. I.; Novotny, M. C.; Bailey, S. R.; Hutchison, J. L.; Green, M. L. H. *Science* **2000**, *289*, 1324.
(18) Wilson, M.; Madden, P. A. *J. Am. Chem. Soc.* **2001**, *123*, 2101.
(19) Talapatra, S.; Migone, A. D. *Phys. Rev. Lett.* **2001**, *87*, 206106.
(20) Kuznetsova, A.; Yates, J. T., Jr.; Liu, J.; Smalley, R. E. *J. Chem. Phys.* **2000**, *112*, 9590.
(21) Kral, P.; Shapiro, M. *Phys. Rev. Lett.* **2001**, *86*, 131.
(22) Ghosh, S.; Sood, A. K.; Kumar, N. *Science* **2003**, *299*, 1042.
(23) Kral, P.; Tomanek, D. *Phys. Rev. Lett.* **1999**, *82*, 5373.
(24) Miyawaki, J.; Kanda, T.; Suzuki, T.; Okui, T.; Maeda, Y.; Kaneko, K. *J. Phys. Chem. B* **1998**, *102*, 2187.
(25) Koga, K.; Gao, G. T.; Tanaka, H.; Zeng, X. C. *Nature* **2001**, *412*, 802.
(26) Maniwa, Y.; Kataura, H.; Abe, M.; Suzuki, S.; Achiba, Y.; Kira, H.; Matsuda, K. *J. Phys. Soc. Jpn.* **2002**, *71*, 2863.
(27) Gogotsi, Y.; Libera, J. A.; Guvenc-Yazicioglu, A.; Megaridis, C. M. *Appl. Phys. Lett.* **2001**, *79*, 1021.
(28) Megaridis, C. M.; Yazicioglu, A. G.; Libera, J. A.; Gogotsi, Y. *Phys. Fluids* **2002**, *14*, L5.
(29) Cornell, W. D.; Cieplak, P.; Bayly, C. I.; Gould, I. R.; Merz, K. M.; Ferguson, D. M.; Spellmeyer, D. C.; Fox, T.; Caldwell, J. W.; Kollman, P. A. *J. Am. Chem. Soc.* **1995**, *117*, 5179.
(30) Verlet, L.; Hansen, J. P. *Mol. Phys.* **1972**, *24*, 1013.
(31) Jorgensen, W. L.; Chandrasekhar, J.; Madura, J. D.; Impey, R. W.; Klein, M. L. *J. Chem. Phys.* **1983**, *79*, 926.
(32) Pearlman, D. A.; Case, D. A.; Caldwell, J. W.; Ross, W. S.; Cheatham, T. E.; Debolt, S.; Ferguson, D.; Seibel, G.; Kollman, P. *Comput. Phys. Commun.* **1995**, *91*, 1.
(33) Berendsen, H. J. C.; Postma, J. P. M.; van Gunsteren, W. F.; DiNola, A.; Haak, J. R. *J. Chem. Phys* **1984**, *81*, 3684.
(34) Darden, T.; York, D.; Pedersen, L. *J. Chem. Phys.* **1993**, *98*, 10089.
(35) Ryckaert, J. P.; Ciccotti, G.; Berendsen, H. J. C. *J. Comput. Phys.* **1977**, *23*, 327.
(36) Dimensions of the cylindrical volume are based on the extent of positional sampling of four methane molecules in the *z* and *r* direction inside the nanotube. The length and radius of the cylinder are chosen at positions where the methane density distribution functions reach one.
(37) Dellago, C.; Naor, M. M.; Hummer, G. *Phys. Rev. Lett.* **2003**, *90*, 105902.
(38) Atkins, P. W. *Physical Chemistry*, 4th ed.; Oxford University Press: Oxford, 1990; chapter 28.2, 848.
(39) Ghosh, T.; García, A. E.; Garde, S. *J. Am. Chem. Soc.* **2001**, *123*, 10997.
(40) Berezhkovskii, A.; Hummer, G. *Phys. Rev. Lett.* **2002**, *89*, 064503.
(41) Bennett, C. H. *J. Comput. Phys.* **1976**, *22*, 245.
(42) Garde, S.; García, A. E.; Pratt, L. R.; Hummer, G. *Biophys. Chem.* **1999**, *78*, 21.
(43) Guillot, B.; Guissani, Y. *J. Chem. Phys.* **1993**, *99*, 8075.
(44) Fu, D.; Libson, A.; Miercke, L. J. W.; Weitzman, C.; Nollert, P.; Krucinski, J.; Stroud, R. M. *Science* **2000**, *290*, 481.
(45) Murata, K.; Mitsuoka, K.; Hirai, T.; Walz, T.; Agre, P.; Heymann, J. B.; Engel, A.; Fujiyoshi, Y. *Nature* **2000**, *407*, 599.
(46) Tajkhorshid, E.; Nollert, P.; Jensen, M. O.; Miercke, L. J. W.; O'Connell, J.; Stroud, R. M.; Schulten, K. *Science* **2002**, *296*, 525.
(47) Zhu, F. Q.; Tajkhorshid, E.; Schulten, K. *Biophys. J.* **2002**, *83*, 154.
(48) Kalra, A.; Garde, S.; Hummer, G. *Proc. Natl. Acad. Sci. U.S.A.* **2003**, *100*, 10175.
(49) Chou, T. *Phys. Rev. Lett.* **1998**, *80*, 85.
(50) Chou, T. *J. Chem. Phys.* **1999**, *110*, 606.
(51) Jirage, K. B.; Hulteen, J. C.; Martin, C. R. *Science* **1997**, *278*, 655.
(52) Mitchell, D. T.; Lee, S. B.; Trofin, L.; Li, N. C.; Nevanen, T. K.; Soderlund, H.; Martin, C. R. *J. Am. Chem. Soc.* **2002**, *124*, 11864.
(53) Humphrey, W.; Dalke, A.; Schulten, K. *J. Mol. Graphics* **1996**, *14*, 33.